SELF-ORIENTED DIFFUSION BASIS FUNCTIONS FOR WHITE MATTER STRUCTURE ESTIMATION

Ramon Aranda, Mariano Rivera

Centro de Investigacion en Matematicas,
Department of Computer Science,
Guanajuato, Gto, Mexico, 36240.

Alonso Ramirez-Manzanares

Universidad de Guanajuato,
Department of Mathematics,
Guanajuato, Gto, Mexico, 36000.

ABSTRACT

We present an extension to the Diffusion Basis Function Model for fitting the *in vivo* brain axonal orientations from Diffusion Weighted Magnetic Resonance Images. The standard Diffusion Basis Functions method assumes that the observed Magnetic Resonance signal at each voxel is a linear combination of a static set of basis functions with equally distributed orientations into the 3D unitary sphere. Our proposal, overcomes the limited angular resolution of the original model by adapting the basis orientations using a sophisticated non-linear optimization procedure. The improvements over the standard Diffusion Basis Functions model estimation by our proposal are demonstrated on the synthetic data-sets used on the 2012 HARDI Reconstruction Challenge.

Index Terms— DW–MRI, Diffusion Tensor, Diffusion Basis Functions, Self–orientation.

1. INTRODUCTION

Nowadays, the water diffusion estimation in cerebral tissue is a non–invasive method for infering axon fiber pathways and connectivity patterns on *in vivo* brains, which are ones of the most challenging goals in neuroimaging. For this aim a special Magnetic Resonance Imaging (MRI) technique named Diffusion Weighted MRI (DW-MRI) is used. The most popular model for representing and analyzing DW-MRI signals is the Diffusion Tensor Magnetic Resonance Images (DT–MRI).

DT–MRI consists of a tensor field that indicates the local orientation of fiber bundles. The tract brain orientation is locally estimated from the eigenvector associated with the largest eigenvalue (main eigenvector) of the estimated tensor. This orientation is known as the Principal Diffusion Direction (PDD). The main limitation of the Diffusion Tensor model is its failure for correctly modeling the signal at voxels with fiber crossings or bifurcations (*partial volume effects*). To better explain the diffusion phenomenon for two or more

fibers, Tuch *et al.* [1] proposed the Gaussian Mixture Model (GMM):

$$S_i = S_0 \sum_{j=1}^{J} \beta_j \exp\left(-bg_i^T T_j g_i\right), \quad (1)$$

where S_0 is the signal without diffusion, b is a constant acquisition parameter, $g_i = [g_{x_i}, g_{y_i}, g_{z_i}]^T$ is an unitary vector which indicates the direction in which the DW-MR signal S_i is measured. T_j is the j-th tensor (a positive definite symmetric 3×3 matrix) with contribution $\beta_j \in (0, 1]$, constrained by $\sum_{j=1}^{J} \beta_j = 1$. J indicates the number of tensors used to explain the signal. In this way, the j-th local fiber orientation (j-th PDD) is estimated from the orientation of the main eigenvector of T_j. For $J = 1$ the model (1) is reduced to the Stejkal–Tanner's equation [2].

In this work, we present a new method to improve the estimation of the PDDs based on the Diffusion Basis Function model for the multi-fiber case. In the following, Section 2 describes the standard Diffusion Basis Function model. Section 3 presents our approach. Section 4 shows the experimental results, followed by our conclusion in Section 5.

2. BRIEF REVIEW OF THE DIFFUSION BASIS FUNCTION MODEL

The solution of (1) is computationally expensive and numerically unstable because requires of the joint estimation of the number of tensors, J, and the solution of a constrained nonlinear optimization problem. For these reasons, Ramirez-Manzanares *et al.* [3] proposed a strategy to solve the inverse problem stated in (1). They avoided the non-linear optimization problem by using a predetermined set of Diffusion Basis Functions (DBF). The basis function are generated from fixed orientations equally distributed on the 3D unitary sphere. Thus, they proposed to model the DW–MR signal as a linear combination of DBFs:

$$S_i \approx \sum_{k=1}^{N} \alpha_k \phi_{i,k}, \quad (2)$$

with $\alpha_k \geq 0$, where the k–th DBF is defined as

$$\phi_{i,k} = S_0 \exp\left(-bg_i^T \bar{T}_k g_i\right). \qquad (3)$$

The coefficient $\phi_{i,k}$ is the diffusion weighted signal value associated to the gradient g_i and the base (fixed) tensor $\bar{T}_k$. The shape of the diffusivity profile, Λ, for every base tensors, $\bar{T}_k$, is assumed constant with $\Lambda = (\lambda_l, \lambda_r, \lambda_r)$, where λ_l is the longitudinal diffusivity and λ_r is the radial diffusivity with $\lambda_l > \lambda_r$ (note that although in this work we use the model in (3) to set the DBFs, it is possible to use others diffusion models, *e.g.*, cylinder restricted diffusion); see for more details in [3]. Hence, by using the DBFs it is possible to solve (1) via a non-negative least-squares (NNLS) problem:

$$\min_{\alpha} \quad U(\alpha) = \|\Phi\alpha - S\|_2^2 \qquad (4)$$
$$\text{subject to} \quad \alpha \geq 0,$$

where $\Phi = \{\phi_{i,k}\}_{i=1,...,M,k=1,...,N}$ and $\alpha = [\alpha_1, ..., \alpha_N]^T$ is the unknown vector of the linear system. By solving (4), the α_i coefficients associated to the DBFs closer to the axon fiber orientations should be nonzero. Since the DBF basis orientations are incomplete in the 3D unity sphere, the number of nonzero α_k values do not always correspond with the actual number of compartment and their associated orientations can be different from the actual ones. Thus, a postprocessing is necessary: to transform the solution from the discrete space (the DBF set) to the continuous 3D orientational space. For this aim, the authors use a heuristic clustering based on the closeness of the fixed basis orientations [3]. It has been reported that this NNLS based DBF approach (hereinafter called standard DBF) is prone to overestimate the number of fibers [4]. Although, other successful methods that use basis functions have also been reported (*e.g.*, see [5, 6]) that the standard DBF approach is an efficient and accurate procedure: it was ranked 3rd best method among the participants of the HARDI reconstruction Challenge in the context of the 2012 IEEE International Symposium on Biomedical Imaging.

As mentioned before, the DBFs are generated from fixed orientations equally distributed into the 3D orientation space and they do not necessary correspond to the actual fiber orientation. For this reason, in next section, we present an extension to reorient the diffusion basis orientations.

3. SELF–ORIENTED DBF MODEL

We define the new DBF formulation as follow:

$$\phi'_{i,k} = S_0 \exp\left(-bg_i^T R(\theta_k) \bar{T}_k R(\theta_k)^T g_i\right), \qquad (5)$$

where R is a 3D reorientation (rotation) matrix defined by the angles $\theta_k = [\theta_{x,k}, \theta_{y,k}, \theta_{z,k}]$, when $\theta_k = [0,0,0]$ this formulation corresponds to eq. (3). In this way, we want to find the angular displacement θ_k to align the PDD of $\bar{T}_k$ with the actual fiber orientation according to the DW-MRI signal. For this aim, we propose to compute the angular displacement by extending the model (4) with (5):

$$\min_{\Theta,\alpha} \quad U(\Theta, \alpha) = \|\Phi(\Theta)\alpha - S\|_2^2 \qquad (6)$$
$$\text{subject to} \quad \alpha \geq 0,$$

where $\Theta = \{\theta_k\}_{k=1,...,N}$ and $\Phi(\Theta) = \{\phi'_{i,k}\}_{i=1,...,M,k=1,...,N}$. The direct minimization of (6) can be complicated because of the constraint on R to be a rotation matrix. Thus, we propose an alternate minimization approach in next subsection.

3.1. Surrogate Model

To simplify the problem stated in (6), we propose to iteratively solve a quadratic program for α and three non-linear programs for Θ until convergence. Solving for α is to resolve the problem in (4), but, to solve for Θ is more complicated. However, we can simplify the problem rewriting R as the product of three rotation matrices around each axis:

$$R(\theta_k) = X(\theta_{x,k})Y(\theta_{y,k})Z(\theta_{z,k}), \qquad (7)$$

where X, Y and Z are the corresponding rotational matrix for the axes x, y and z, respectively. Then, we write each rotation matrix in terms of the cosine directors:

$$X(\theta_{x,k}) = X_k = \begin{bmatrix} 1 & 0 & 0 \\ 0 & \cos(\theta_{x,k}) & -\sin(\theta_{x,k}) \\ 0 & \sin(\theta_{x,k}) & \cos(\theta_{x,k}) \end{bmatrix}, \qquad (8)$$

$$Y(\theta_{y,k}) = Y_k = \begin{bmatrix} cos(\theta_{y,k}) & 0 & \sin(\theta_{y,k}) \\ 0 & 1 & 0 \\ -\sin(\theta_{y,k}) & 0 & \cos(\theta_{y,k}) \end{bmatrix}, \qquad (9)$$

$$Z(\theta_{z,k}) = Z_k = \begin{bmatrix} \cos(\theta_{z,k}) & -\sin(\theta_{z,k}) & 0 \\ \sin(\theta_{z,k}) & \cos(\theta_{z,k}) & 0 \\ 0 & & 0 \end{bmatrix}. \qquad (10)$$

Moreover, if we constrain such rotational angles in θ_k to be small, then we can use the following approximations:

$$X_k \approx \begin{bmatrix} 1 & 0 & 0 \\ 0 & 1 & -\theta_{x,k} \\ 0 & \theta_{x,k} & 1 \end{bmatrix}, \qquad (11)$$

$$Y_k \approx \begin{bmatrix} 1 & 0 & \theta_{y,k} \\ 0 & 1 & 0 \\ -\theta_{y,k} & 0 & 1 \end{bmatrix}, \qquad (12)$$

$$Z_k \approx \begin{bmatrix} 1 & -\theta_{z,k} & 0 \\ \theta_{z,k} & 1 & 0 \\ 0 & 0 & 1 \end{bmatrix}. \qquad (13)$$

Thus, we can write (5) as

$$\phi'_{i,k} = S_0 \exp\left(-bg_i^T X_k Y_k Z_k \bar{T}_k Z_k^T Y_k^T X_k^T g_i\right). \qquad (14)$$

Now, if only one of the rotations X, Y or Z is applied at each time, then the problem is reduced to three problems easier-to-solve. For instance, to solve the angular displacement in X_k, we fix the values for Y_k, Z_k. Thus, let $\Theta_w = \{\theta_{w,k}\}_{k=1,2,...N}$ be the set of angular rotations in the w (with $w = z, y$ or z) axis for the basis functions. Then, the cost function associated to the angular displacement Θ_w can be written as:

$$U(\Theta_w) =$$
$$\sum_i \left[S_0 \sum_k \alpha_k \exp\left(c_{i,1}^w \theta_{w,k}^2 + c_{i,2}^w \theta_{w,k} + c_{i,3}^w\right) - S_i \right]^2, \tag{15}$$

where the α_k's values are the solution of (4) and they are fixed at this stage, c_i^w is a constant vector that depends on the selection of w and results of applying algebraic factorization on $-b g_i^T X_k Y_k Z_k \bar{T}_k Z_k^T Y_k^T X_k^T g_i$. For instance, if $w = x$ the others parameters $\theta_{y,k}$ and $\theta_{z,k}$ are considered constant values. Hence, the reorientation angles are computed by the joint solution of:

$$\min_{\Theta_x} \quad U(\Theta_x) \quad \text{s. t. } |\theta_{x,k}| \leq u, \tag{16}$$

$$\min_{\Theta_y} \quad U(\Theta_y) \quad \text{s. t. } |\theta_{y,k}| \leq u, \tag{17}$$

$$\min_{\Theta_z} \quad U(\Theta_z) \quad \text{s. t. } |\theta_{z,k}| \leq u, \tag{18}$$

where the upper bound u constrains the rotations to be small such that the approximations of the sines and cosine in (11),(12) and (13) are valid; we set $u = 8$ degrees.

Through experimentation, we note that a MRI signal corresponding with a tensor with large diffusivity profile causes an activation of two or even three DBF signals in order to have the best fitting. Also, we observed that the diffusion profile of the basis is important to compute the optimal solution; *i.e.*, basis functions with small radial diffusivity, λ_r, are prone to be trapped on local minimum. As was reported by [7], we also noted that a more isotropic DBF result in sparser representations. For these reasons, after a local minimum is reached, we augment the DBF set by adding a new DBFs aligned with the normalized vectorial addition of each pair or triad of diffusion directions such that $\alpha > 0$. Further, we increase λ_r for all the DBF set by using a factor $\mu > 1$. Algorithm 1 resumes our self–oriented DBF model. Note that, although we allow only small orientation changes at each iteration of the internal loop, the effect of several iterations can produce large orientation changes. Also, note that we solve (16)–(18) only for the $\theta_{w,k}$ such that $\alpha_k > 0$ and not for the complete DBF set.

4. RESULTS

Here, we compare the performance of our proposal vs. the standard DBF model reviewed in section 2. The experiments were conducted on the publicly available data set used in the 2012 HARDI Reconstruction Challenge (for

---

Algorithm 1 Self–Oriented DBF Model.

Require: Given a initial set $\mathbb{T}^0 = \{\bar{T}_k^0\}$ for $k = 1, 2, ..., N$ with initial diffusivity profile $\Lambda^0 = \{\lambda_l^0, \lambda_r^0, \lambda_r^0\}$, $\mu > 1$ (typically $\mu = 1.15$)

1: Set $s = 0$;
2: **repeat**
3:     Set $\Phi(\Theta)^0$ with (3) using $\mathbb{T}^0$ and $t = 0$
4:     **repeat**
5:         Compute α^t using $\Phi(\Theta)^t$ by solving (4);
6:         Assign $\mathbb{T}^t = \{\bar{T}_k^t | k : \alpha_k^t > 0\}$;
7:         $N = |\mathbb{T}^t|$;
8:         Set $X_k^t = Y_k^t = Z_k^t = I$ for each $\bar{T}_k^t \in \mathbb{T}^t$;
9:         Update $X_{1:N}^{t+1}$ solving (16) with $Y_{1:N}^t$, $Z_{1:N}^t$ fixed;
10:       Update $Y_{1:N}^{t+1}$ solving (17) with $X_{1:N}^{t+1}$, $Z_{1:N}^t$ fixed;
11:       Update $Z_{1:N}^{t+1}$ solving (18) with $X_{1:N}^{t+1}$, $Y_{1:N}^{t+1}$ fixed;
12:       Update $\mathbb{T}^{t+1} = \{\bar{T}_k^{t+1} = X_k^{t+1} Y_k^{t+1} Z_k^{t+1} \bar{T}_k^t Z_k^{t+1^T} Y_k^{t+1^T} X_k^{t+1^T} : \bar{T}_k^t \in \mathbb{T}^t\}$;
13:       Update $\Phi(\Theta)^{t+1}$ with (3) using $\mathbb{T}^{t+1}$;
14:       $t = t + 1$;
15:     **until** a local minimum is reached
16:     Update $\mathbb{T}^t$ by adding tensors with PDDs equal to the normalized sum of every pair and triad of PDDs in the set $\mathbb{T}^t$ and with diffusivity profile Λ^s;
17:     Increase the diffusivity profile $\Lambda^{s+1} = \{\lambda_l^s, \mu\lambda_r^s, \mu\lambda_r^s\}$ for each $\bar{T}_k^t \in \mathbb{T}^t$;
18:     Set $\mathbb{T}^0 = \mathbb{T}^t$ and $s = s + 1$;
19: **until** convergence

---

more details visit `http://hardi.epfl.ch/static/events/2012_ISBI/index.html`). We show the results using the data set called *Testing_IV*. The set consists of 9100 synthetic independent signals, that is to say, spatially unstructured with 100 voxels with only one compartment and 9000 voxels with two compartments crossing at different degrees [see Figure 1(a)]. We used an acquisition scheme of 64 diffusion orientations and a b-value $= 2000$ with different Signal-Noise-Ratios (SNR). For the standard DBF 129 base tensors were used and for our approach 256. These values were set according to the best performance of each method.

To evaluate the results, we take into account two criteria: the angular error and the number of wrongly estimated compartments. To compute the angular error we match estimated PDDs with the actual PDDs such that we have the best possible assignment. We assume that only p assignments are performed, where p is the minimum between the estimated number of compartments and the actual number of compartments. Thus, the angular error is computed as the average angular error between paired PDDs. Figure 1(b) compares the angular errors of our approach versus the errors of the standard DBF. One can see that our proposal effectively reduces the average and variance of the angular error *w.r.t.* the standard DBF. By the other hand, the number of wrongly es-
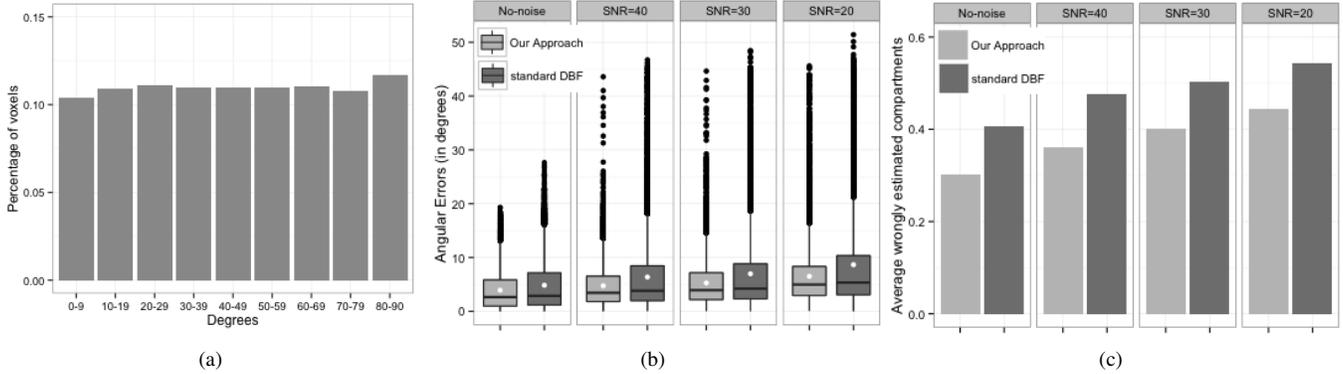
Fig. 1. (a) Percentage of crossing compartments by angles. (b) Boxplot of all angular errors for the *Testing_IV* data with different SNR values. The white point in boxplots depicts the average angular error. (c) Average compartment estimation error on the *Testing_IV* data for different SNR values.

timated compartments equals 1 if the estimated number of compartments in a voxel is different from the actual number of compartments and zero otherwise. This error measure includes both underestimations and overestimations. Figure 1(c) shows the average of the wrongly estimated compartments for all the voxels. Note that our proposal consistently reduces the number of wrongly estimated compartments. One disadvantage of our proposal is the computational cost: standard DBF takes around 10 minutes for processing the *Testing_IV* data set (9100 voxels), our method takes around 3 hours.

5. CONCLUSIONS

We presented an algorithm that reorients the diffusion directions of a DBF set. Our method overcomes the limitation of the standard DBF model: the orientations are fixed, and thus they do not necessarily correspond to the actual fiber orientation. To adjust the diffusion orientations can be complicated, for this reason, we simplified the problem by proposing an alternate minimization approach that consists of iteratively solving a sequence of a quadratic program and three non–lineal programs. Our proposal improves one of the best methods for analyzing DW-MRI data (according to the 2012 HARDI Reconstruction Challenge) by reducing the variability and the average of the angular error, as well as the error in the estimated number of compartments per voxel. Additionally, in our experiments we noted that in most cases of solutions with large angular error, the actual fiber orientation can be parallel to the vectorial addition of every pair or triad of the resulting DBF orientations. For this reason, we added those new diffusion directions to the BDF set and we heuristically increase the radial diffusivity for each tensor in the DBF set in order to improve the model fitting. As a future work, we are studying alternative approaches to estimate better the diffusivity profile and, accordingly, the diffusion orientations.

6. REFERENCES

[1] David S. Tuch, Timothy G. Reese, Mette R. Wiegell, Nikos Makris, John W. Belliveau, and Van J. Wedeen, "High angular resolution diffusion imaging reveals intravoxel white matter fiber heterogeneity," *Magn. Reson. Med.*, vol. 48, no. 4, pp. 577–582, 2002.

[2] Peter J. Basser, James Mattiello, and Denis Lebihan, "MR diffusion tensor spectroscopy and imaging," *Biophysical Journal*, vol. 66, pp. 259–267, 1994.

[3] Alonso Ramírez-Manzanares, Mariano Rivera, Baba C. Vemuri, Paul Carney, and Thomas Mareci, "Diffusion basis functions decomposition for estimating white matter intravoxel fiber geometry," *IEEE Trans. Med. Imag.*, vol. 26, no. 8, pp. 1091–1102, 2007.

[4] Alonso Ramirez-Manzanares, Philip A Cook, Matt Hall, Manzar Ashtari, and James C Gee, "Resolving axon fiber crossings at clinical b-values: An evaluation study.," *Med Phys*, vol. 38, no. 9, pp. 5239, 2011.

[5] J-Donald Tournier, Fernando Calamante, and Alan Connelly, "Robust determination of the fibre orientation distribution in diffusion MRI: Non-negativity constrained super-resolved spherical deconvolution," *NeuroImage*, vol. 35, no. 4, pp. 1459–1472, May 2007.

[6] Bennett A. Landman, John A. Bogovic, Hanlin Wan, Fatma El Zahraa ElShahaby, Pierre-Louis Bazin, and Jerry L. Prince, "Resolution of crossing fibers with constrained compressed sensing using diffusion tensor mri.," *NeuroImage*, vol. 59, no. 3, pp. 2175–2186, 2011.

[7] Omar Ocegueda and Mariano Rivera, "Dynamic diffusion basis functions for axon fiber structure estimation from DW-MRI," in *MICCAI Workshop on Computational Diffusion MRI (CDMRI'12)*, 2012, pp. 90–101.